

# Pyrolysis of Meteoritic Organics and Fragmentation of Cosmic Dust during Atmospheric Entry

John Plane<sup>1</sup>, David Bones<sup>1</sup>, Alexander James<sup>1</sup>, Benjamin Murray<sup>1</sup>, Juan Diego Carrillo-Sánchez<sup>2</sup>, Graham Mann<sup>1</sup>, and Simon Connell<sup>1</sup>

<sup>1</sup>University of Leeds

<sup>2</sup>NASA Goddard Space Flight Center

November 22, 2022

## Abstract

We have developed a new experimental system to study the pyrolysis of the refractory organic constituents in cosmic dust. Pyrolysis is observed by mass spectrometric detection of CO<sub>2</sub> and SO<sub>2</sub>, and starts from around 850 K. The time-resolved kinetic behaviour is consistent with two organic components – one significantly more refractory than the other, which probably correspond to the insoluble and soluble organic fractions, respectively. The laboratory results are then incorporated into the Leeds Chemical Ablation Model (CABMOD), which is used to predict the conditions under which organic pyrolysis should be detectable using a high performance/large aperture radar. It has been proposed that loss of the organics leads to fragmentation of cometary dust particles into micron-sized fragments. If fragmentation of dust particles from Jupiter Family and Halley Type Comets does occur to a significant extent, there are several important implications: 1) slow-moving particles, particularly from Jupiter Family Comets, will be undetectable by radar, so that the total dust input to the atmosphere may be considerably larger than current estimates of 20 – 50 tonnes per day; 2) experiments at Leeds show that meteoritic fragments are excellent ice nuclei for freezing stratospheric droplets in the polar lower stratosphere, producing polar stratospheric clouds which activate chlorine and cause ozone depletion; and 3) the measured accumulation rates of meteoric smoke particles, micrometeorites and cosmic spherules in the polar regions can now be explained self-consistently.

# Pyrolysis of Meteoritic Organics and Fragmentation of Cosmic Dust during Atmospheric Entry

John M. C. Plane<sup>1</sup>, David L. Bones<sup>1</sup>, Alexander D. James<sup>1</sup>, Benjamin J. Murray<sup>2</sup>, Juan Diego Carrillo-Sánchez<sup>1,4</sup>, Graham W. Mann<sup>2</sup> and Simon D. A. Connell<sup>3</sup>

<sup>1</sup>School of Chemistry, University of Leeds, Leeds, U.K.; <sup>2</sup>School of Earth and Environment, University of Leeds; <sup>3</sup>School of Physics and Astronomy, University of Leeds; <sup>4</sup> NASA Goddard Space Flight Center, Maryland.

## Abstract

We have developed a new experimental system to study the pyrolysis of the refractory organic constituents in cosmic dust. Pyrolysis of meteoritic fragments is observed by mass spectrometric detection of CO<sub>2</sub> and SO<sub>2</sub>, and starts from around 850 K. The time-resolved kinetic behaviour is consistent with two organic components – one significantly more refractory than the other, which probably correspond to the insoluble and soluble organic fractions, respectively. The laboratory results are then incorporated into the Leeds Chemical Ablation Model (CABMOD), which is used to predict the conditions under which organic pyrolysis should be detectable using a high performance/large aperture radar. Atomic force microscopy was used to examine how the strength of the particles changed before and after organic pyrolysis. This showed that although the particles became more brittle, they also became slightly harder, withstanding stresses that are at least 3 orders of magnitude higher than would be encountered during atmospheric entry. This suggests that most cosmic dust particles (radius < 100 μm) will not fragment in the atmosphere as a result of organic pyrolysis.

## Introduction

Good progress has been made in the past decade developing models of meteoric ablation. These are now able to predict the ablation rates of individual elements from a dust particle of specified mass, velocity and entry angle. These elements include a range of metals (Fe, Mg, Na etc.), Si and P (Bones et al., 2019; Carrillo-Sanchez et al., 2020). These models have been tested in the laboratory using meteoric ablation simulators (Gómez Martín et al., 2017; Thomas et al., 2017; Bones et al., 2019; ). However, to date the effect of the pyrolysis of carbon and sulfur compounds in cosmic dust at temperatures below 1300 K (i.e. prior to melting), which can potentially lead to *meteoric fragmentation*, has not been considered in detail. In the present study we report measurements of the rates of pyrolysis of C and S in meteoritic fragments, and also determine the changes in tensile strength of the particles. We use these results to examine the likelihood that organic pyrolysis leads to fragmentation during atmospheric entry, and to predict whether organic pyrolysis could be observed by a High Performance Large Aperture radar.

## Evidence for organic "glue" in cosmic dust

When meteoroids fragment, it is reasonable to assume that some component or components of the meteoroid are responsible: either pressurized pockets of gas explosively break the particle apart, or volatile compounds evaporate or pyrolyse, thereby weakening the matrix of the meteoroid. The tendency of fragments from large meteoroids to retain a similar trajectory to the parent body suggests the latter scenario is more typical. Generally, meteoroids consist of primitive grains surrounded by a matrix. For instance, interplanetary dust particles (IDPs) captured in the stratosphere include porous aggregates of silicate grains surrounded by an organic carbon mantle (Flynn et al., 2013; Kimura et al., 2020). If this carbon were to pyrolyse as the particle heats on entry to the atmosphere, the aggregates could fall apart into smaller grain clusters. The meteor would only have to reach moderate temperatures of around 900 K to lose most of the organic carbon.

Terrestrial meteorites contain a huge variety of organic carbon, ranging from soluble, volatile hydrocarbons (termed Soluble Organic Matter, SOM) to large, refractory, insoluble macromolecular polycyclic aromatic hydrocarbon (PAH) compounds similar to the terrestrial kerogen found in oil shales. This latter fraction, termed Insoluble Organic Matter (IOM), accounts for about 70% of the organic carbon in a typical CM or CI meteorite. Many compounds are highly functionalised with a number of carbonyl groups. The bulk of the compounds appear to be functionalised single cycle aromatic molecules (Cody et al., 2011). In general, the IOM in the more primitive meteorites (CM, CI, CR) is more primitive than the IOM in IDPs; the variety of the soluble compounds is also huge – 46 000 compounds of different chemical formula were isolated from Murchison (Alexander et al., 2017).

The types of carbon compound in the organic mantles of Chondritic Porous IDPs are in general highly conjugated, aromatic groups but with significant carbonyl features and some CH<sub>3</sub> and CH<sub>2</sub> features (Schramm et al., 1989; Flynn et al., 2004). The organic matter often varies hugely even within the same particle. The carbon content of IDPs is around 12% (Thomas et al., 1994). This is significantly more than the 2% found in a primitive carbonaceous chondrite meteorite and closer to the carbon content of cometary samples.

The Stardust mission to Wild2 returned samples that included carbon compounds with a resemblance to those found in IDPs. In general, the H/C ratio was relatively high (close to 1), indicating aliphatic compounds rather than aromatic compounds, although small amounts of the latter were also evident (Clemett et al., 2010). Rosetta measurements confirm the picture of aggregates bound together by an organic mantle (Kimura et al., 2020). The organic and silicate phases were “intimately mixed”. The organic phase accounted for at least 45% of the total – far more than observed in IDPs or meteorites.

Rosetta particles are very diverse, but appear to be aggregates of sub units about 10 μm in radius, with aggregate tensile strengths in the 1000s of Pa region (Hornung et al., 2016).

### **Previous laboratory work**

Several previous experiments have investigated the effect of flash heating on micrometeoroids. Often, the emphasis is on mineralogical changes to the particle (Nozaki et al., 2006). Outgassing of volatiles has also been studied using linear temperature ramps or stepped pyrolysis studies (Court and Sephton, 2009). A recent study where insoluble organic matter (IOM) extracts (from the Cold Bokkeveld CM2 meteorite) were flash heated showed

that at temperatures above 900 K significant alteration to the IOM composition occurred, with evidence of more ordered aromatic groups and a loss of carbonyl functional groups (Riebe et al., 2020).

## Laboratory Experiments on Pyrolysis and Fragmentation

### Pyrolysis kinetics

The new Meteoric Ablation Simulator (MASI) developed for this study is illustrated in Figure 1. Inside the chamber is a heated platform (red block in Fig. 1). Samples are held in a hopper above the platform until it reaches the required temperature, at which point the sample is released and funnelled onto the hot surface.

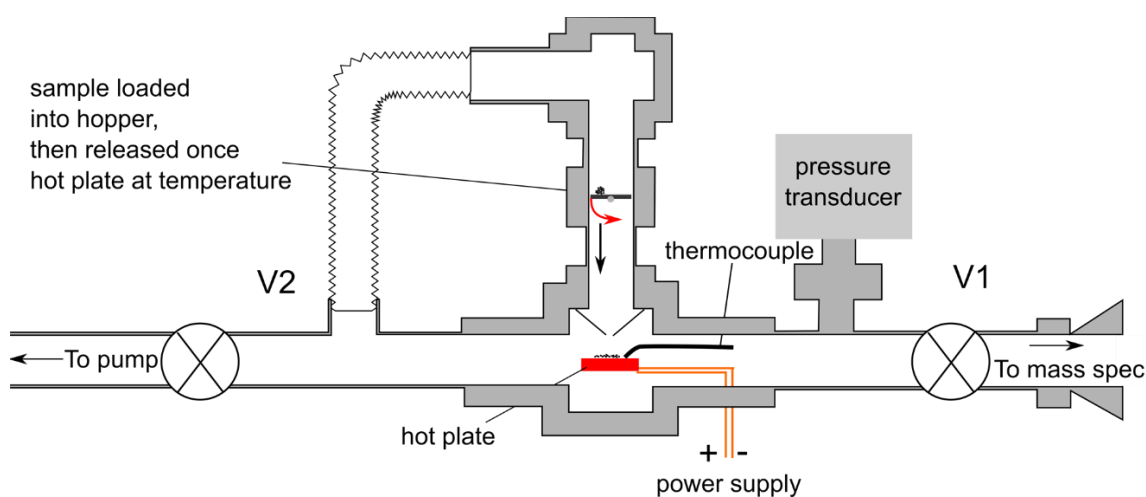


Figure 1. Schematic diagram of the ablation chamber

The platform consists of Omega bond cement, with a length of coiled NiChrome wire embedded in it so that the surface can be resistively heated to a maximum temperature of 1600 K. The chamber can be pumped down to around 0.1 Pa.

A Hiden HPR60 quadrupole mass spectrometer was used to analyse the gases emitted from the hot particles. A single mass could be monitored at a rate of 6 Hz. Alternatively, scanning from 10 - 120 amu could be carried out at 0.07 Hz. Gases produced in the MASI chamber were pumped past the orifice of the mass spectrometer using an Edwards E2M80 rotary pump backed by a roots blower. This ensured that any gas produced was sampled by the mass spectrometer on a timescale of a few milliseconds.

The meteorite chosen as the primary micrometeorite proxy was a carbonaceous chondrite of CM2 classification called Jbilet Winselwan (JW). This is a relatively primitive, carbon rich meteorite that is the closest available match to cometary dust. Cometary dust accounts for up to 90% of the meteorites entering the Earth's atmosphere (Carrillo-Sánchez et al., 2016) and is expected to have a composition similar to primitive chondrites, albeit less dense and with higher carbon content. To conserve our limited supply of JW, a sample of oil shale was obtained from the British Geological Survey. The organic carbon in oil shale is largely in the

form of kerogen, as in meteorites. The pyrolysis of carbon from oil shale has also been extensively studied, providing a useful benchmark.

JW is notable among CM2 meteorites for its lack of carbonates, which in turn suggests little hydrous alteration. Otherwise, in terms of elemental composition, general mineral compositions and oxygen isotope ratios it is typical of the CM2 category (Friend et al., 2018).

The other available meteorite sample was the CV3 carbonaceous chondrite Allende, which is significantly lower in carbon content than JW. Allende has been well studied since its fall in Mexico in 1969 (Jarosewich, 1990).

The oil shale and the meteorite samples were ground to a coarse powder in an agate mortar and pestle, then size selected by an Endecott test sieve. This results in bins of particles of average radius 36, 64 and 100  $\mu\text{m}$  ( $\pm 50\%$ ).

## **AFM yield stress tests**

Atomic force microscopy was performed using a Nanoscope 8 Multimode (Bruker) on samples of oil shale and JW meteorite, both 'fresh' (unheated) and heat-treated (to  $\sim 900$  K). The particles were mounted on metal stubs. Yield stress tests were conducted on a minimum of 4 regions of 6-10 particles per sample. Each area was only probed once, as only 5 repeated measurements in the same location results in a compacted hole in the surface with no measurable indentation and high adhesion. The AFM is equipped with a top down camera for location of the probe. FESPA AFM probes (Bruker Probes, nominal spring constant of  $2.8 \text{ N m}^{-1}$ ) were used in contact mode, under air.

The probe tip is at the end of a cantilever. The spring constant of the cantilever was measured using the thermal noise method (plotting the thermally driven deflection fluctuations as a function of frequency), and the Sader method (using knowledge of probe geometry and materials together with its resonant frequency). The spring constants were in the range  $1.2$ - $2.6 \text{ N m}^{-1}$ , and the values obtained by the two methods were typically within 5% of one another.

The surface stress generated by the tip depends on the normal force and the tip radius, and this value can change with wear. The tip radius was checked by running the AFM in Peak Force – Quantitative Nanomechanical Mapping (PF-QNM) mode on a low density polyurethane standard sample of known modulus. With all other parameters calibrated, the tip radius is the only free adjustable parameter to achieve the correct elastic modulus. Force indentation curves were controlled using a relative trigger. This was generally set to 100 nN, but if this force was not sufficient to cause the surface to indent or yield it was increased in further 100 nN increments. The samples were studied over a period of 2 months, and multiple probes were used for the same samples, introducing the maximum amount for repeatability across the different probes used. Data was analysed using Nanoscope Analysis v9.1 (Bruker).

## **Experimental Results and Discussion**

### **Mass resolved gas analysis from linear temperature ramps**

Samples of the two meteorites were subjected to linear temperature ramps from 293 K to 1300 K. Unambiguous releases of carbon- and sulfur-containing compounds were observed. Other species, including potential nitrogen-containing compounds and chlorine were possibly also produced, but cannot be identified with certainty.

Figure 2a shows the ablation of four different carbon compounds from the JW meteorite. Masses 12 and 44 a.m.u show clear trends of increasing ablation at high temperature, with some hint of a maximum before the linear ramp is terminated at about 1350 K. Ablation starts at around 800 K. Mass 12 is unambiguously C and the correspondence of its profile with mass 44 lends confidence to the assignment of CO<sub>2</sub> to mass 44, although it is possible there are contributions from other carbon-containing species C<sub>3</sub>H<sub>8</sub> and C<sub>2</sub>H<sub>4</sub>O. Mass 28 is likely CO, although N<sub>2</sub> and C<sub>2</sub>H<sub>4</sub> cannot be ruled out. CO<sub>2</sub> fragments into C and CO during electron impact ionisation, with both fragments about 10% abundance of the parent peak.

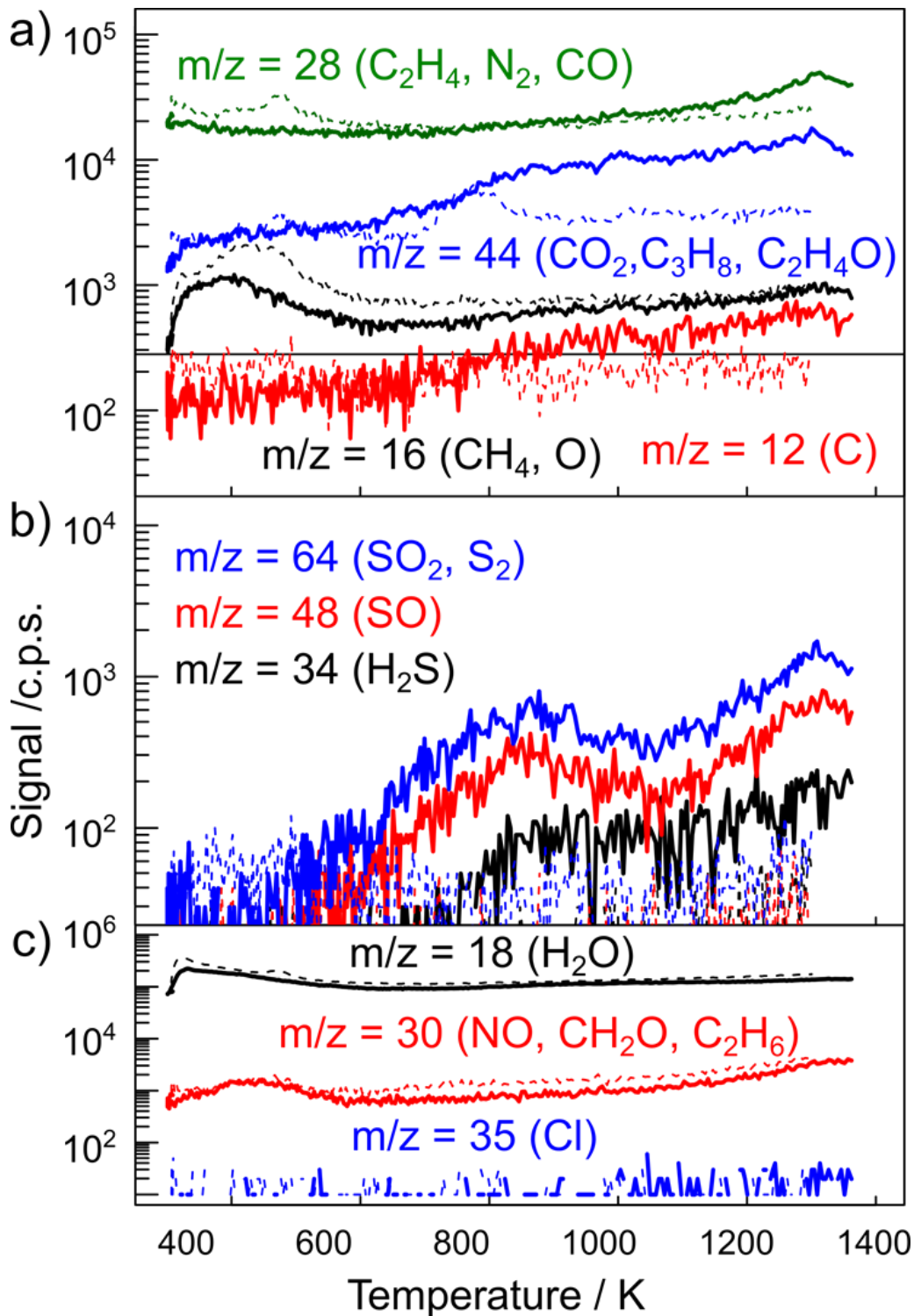


Figure 2. Signal profiles of gases emitted during a linear heating ramp of 100  $\mu\text{m}$  particles from the JW meteorite. Dotted lines: blank profiles (i.e. with no sample loaded). a) Profiles attributed to C containing compounds. b) Profiles attributed to S containing compounds. c) Other profiles.

The mass profiles of three likely sulfur compounds – masses 34, 48 and 64 are depicted in Figure 2b. Mass 64 could be  $\text{S}_2$ , but is much more likely  $\text{SO}_2$  as a sulfide oxidation product. This is confirmed by the mass 64 profile tracking that of mass 48, due to  $\text{SO}_2$  fragmenting to form SO. Mass 34 exhibits a slightly different profile. It is likely to be  $\text{H}_2\text{S}$ , evaporating

directly from the meteorite. All of these likely sulfur profiles show a double peak, initially peaking around 900 K (slightly later for H<sub>2</sub>S) followed by a rise to a maximum at 1300 K, before the linear ramp was halted at a temperature of 1350 K.

Sulfur is present in carbonaceous chondrites at around 2 - 3 wt% (Court and Sephton, 2011), somewhat higher than the carbon content. The total sulfur released in the linear ramp depicted in Figure 2, however, was approximately seven times lower than the total carbon (once the relative ionization cross sections of CO<sub>2</sub>, SO<sub>2</sub> and H<sub>2</sub>S had been corrected for). It is clear that much more carbon than sulfur is emitted at temperatures lower than 1300 K. Sulfates present in the meteorite samples (typically CaSO<sub>4</sub> and MgSO<sub>4</sub>) would not decompose at temperatures below 1300 K.

Figure 2c also shows the mass profiles of masses 30 and 35. Mass 35 is not an isotopologue of H<sub>2</sub>S because its abundance would be less than 1% of the H<sub>2</sub>S signal and hence not detectable. The most likely candidate is Cl. Mass 30 is ambiguous.

### Pyrolysis rates

The rates of carbon pyrolysis from the meteoroid proxies were measured from the time-resolved production of m/z = 44, corresponding to CO<sub>2</sub>, which is the major pyrolysis product. The maximum rate of CO<sub>2</sub> production, normalised to the total CO<sub>2</sub> ablated, was extracted from each experiment. The Arrhenius plots in Figure 3a show that the pyrolysis rates for 100 μm particles from JW and Allende are very similar (within the 1σ error).

Given that CO<sub>2</sub> is the major carbon-containing product, the fugacity of O<sub>2</sub> in the chamber could then be a rate limiting factor. However, as shown in Figure 3b the Arrhenius plots with and without added O<sub>2</sub> are near-identical. **This result implies that the oxygen reacting with the organic C is internal to the particles.** There is also no clear trend in the Arrhenius parameters with particle size (Figure 3c), **which indicates that the release of CO<sub>2</sub> from the particles is not diffusion-controlled.** Unsurprisingly, the oil shale particles produced notably different Arrhenius parameters (Figure 3d).

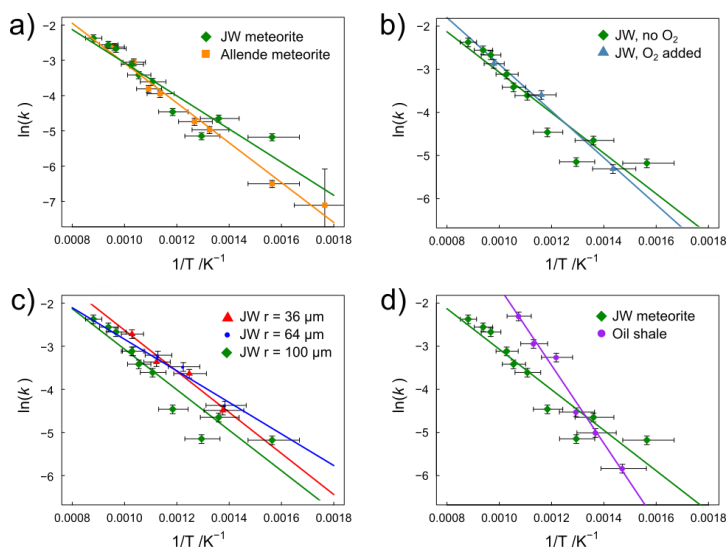


Figure 3. (a) Arrhenius plots for carbon pyrolysis in particles from the Jbilet Winselwan (CM2) and Allende (CV3) meteorites. (b) Arrhenius plots for pyrolysis from JW particles in

the presence of no added O<sub>2</sub> (background pO<sub>2</sub> = 0.026 Pa) and added O<sub>2</sub> (pO<sub>2</sub> = 0.54 Pa). (c) Arrhenius plots for CO<sub>2</sub> production from JW particles of different average sizes. (d) Arrhenius plots of pyrolysis from JW and terrestrial oil shale samples. The solid lines are linear regression fits through each set of data.

### Yield stress measurements

The yield stress of the particles did not change significantly after pyrolysis. Both the oil shale and JW particles tended to become harder after pyrolysis at 925 K; however, they also become more brittle (i.e., when the yield pressure was reached, the material would then give way with a much deeper load drop). The lowest initial yield points, taken from the distribution of all particles examined, were:

Oil Shale (fresh)	3.0 MPa
Oil Shale (925 K)	3.1 MPa
JW (fresh)	1.2 MPa
JW (925 K)	1.9 MPa

Note that these stresses are *much* larger than the 500 Pa - 1 kPa pressures encountered by cosmic dust particles during atmospheric entry. **We therefore conclude that organic pyrolysis is unlikely to cause fragmentation during the atmospheric entry of cosmic dust particles in the common size range below  $r = 100 \mu\text{m}$ . This would certainly be the case for more dense asteroidal particles, and probably apply to most cometary particles apart from the most fragile.**

## Atmospheric Modelling of Carbon Ablation and Radar Cross Sections

### Organic pyrolysis model

It is evident from the time-resolved CO<sub>2</sub> emission profiles that at least two carbonaceous components are involved, one relatively volatile and the other relatively refractory. These probably correspond to the SOM and IOM components in IDPs and meteorites (see Introduction). We therefore constructed a kinetic model which included two terms to account for the fraction of carbon ablated:

$$\text{Fraction} = f_{\text{SOM}}(1 - e^{-k_{\text{SOM}} t}) + f_{\text{IOM}}(1 - e^{-k_{\text{IOM}} t})$$

where  $f_{\text{SOM}}$  and  $f_{\text{IOM}}$  are the fraction of soluble and insoluble carbon in the particles, and  $k_{\text{SOM}}$  and  $k_{\text{IOM}}$  are the first-order rate constants for pyrolysis. The finite rate of heat transfer from the surface to the particle was included to account for the initial lag in ablation of carbon seen in the experimental MASI profiles (Figure 4).

The model parameters were manually adjusted to get the best match between the modelled and experimental profiles (Figure 4). This yields:

$$f_{\text{SOM}} = 0.59; f_{\text{IOM}} = 0.41$$

$$k_{\text{SOM}} = 2.5 e^{-(2100/T)} \text{ s}^{-1}; k_{\text{IOM}} = 2.9 e^{-(3700/T)} \text{ s}^{-1}$$

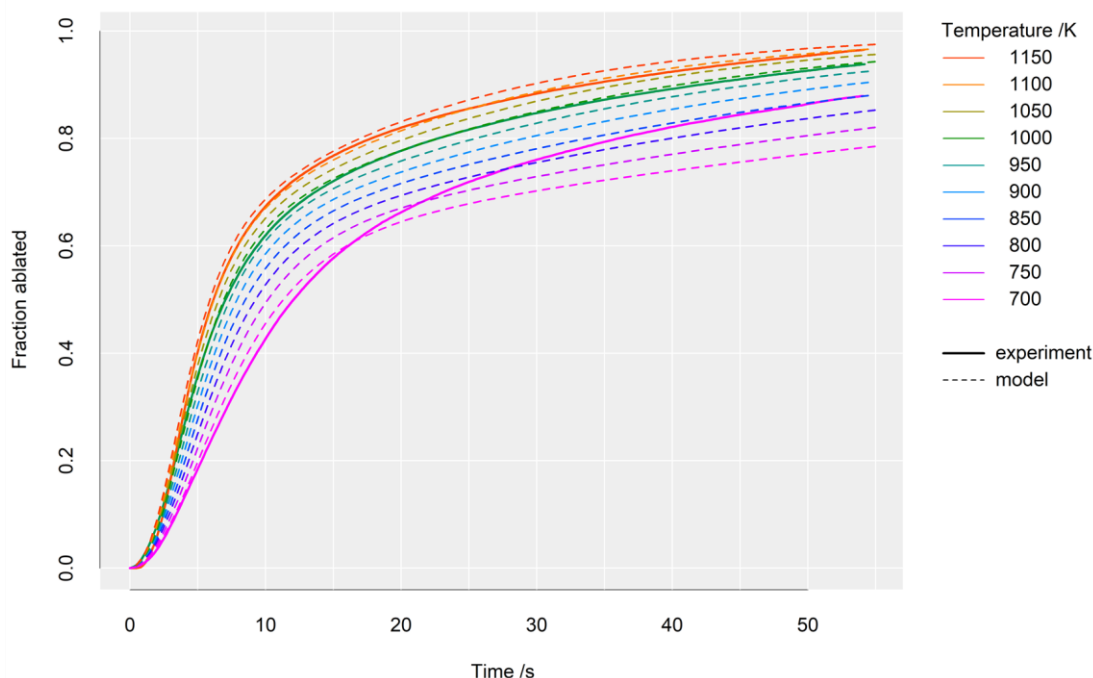


Figure 4. Examples of the time-resolved ablation of  $\text{CO}_2$  at three different temperatures for JW meteorite particles ( $r = 100 \mu\text{m}$ ). The ordinate axis - Fraction ablated - refers to fraction of carbon (SOM and IOM) ablated at the hot plate specified temperature. The experimental profiles are the solid lines, and the model fits are shown with dashed lines.

These rate coefficients can now be used in the CABMOD ablation model (Carrillo-Sanchez et al., 2020) to predict the atmospheric ablation profile of organic carbon, assuming the SOM/IOM fraction obtained above. We are interested to see whether the predicted release of  $\text{CO}_2$  at temperatures above 800 K would be detectable by a High Performance Large Aperture (HPLA) radar, taking the Arecibo radar as an example. We consider here a  $20 \mu\text{g}$  particle ( $r = 125 \mu\text{m}$ ), entering the atmosphere at  $35^\circ$  to the zenith, at speeds of 15, 30 and  $60 \text{ km s}^{-1}$ . The ionization probability of the ablated  $\text{CO}_2$  is calculated using the formalism in

Janches et al. (2017), and the resulting radar S/N for Arecibo using the method described by Janches et al. (2014).

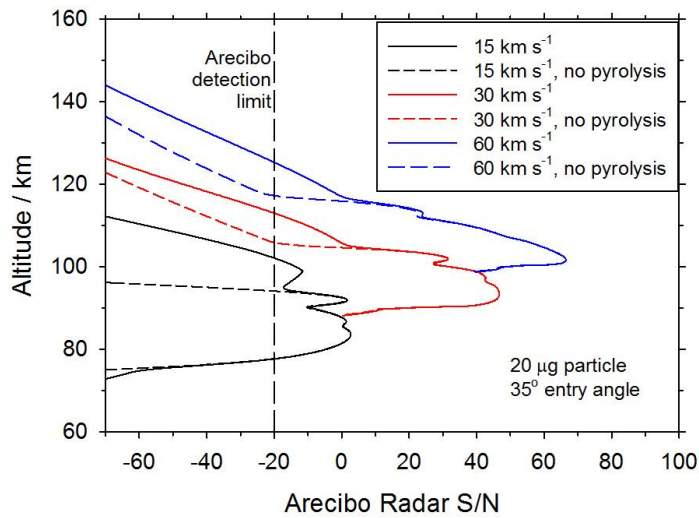


Figure 5. The radar S/N predicted as a function of height for the Arecibo HPLA radar observing a 20  $\mu\text{g}$  cosmic dust particle entering the atmosphere at three different velocities. The solid lines include  $\text{CO}_2$  ablation as well as metals, whereas the dashed lines show the case where no organic pyrolysis occurs.

Inspection of Figure 5 shows that the ablation of  $\text{CO}_2$  should make a significant difference to the topside of the radar profile. However, it is only for the slowest particles ( $15 \text{ km s}^{-1}$ ) that a clear detached layer is observed at around 100 km (the narrow layer at 92 km is due the ablation of Na and K). The detection limit for the Arecibo radar is about -20 dB, **so the organic caused by organic pyrolysis should be observable with HPLA radars.**

**Acknowledgments.** This work was funded by the UK Natural Environment Research Council (grant number NE/R011222/1). We thank the British Geological Survey for providing the oil shale sample.

## REFERENCES

Alexander, C. M. O., Cody, G. D., De Gregorio, B. T., Nittler, L. R., Stroud, R. M. (2017), The nature, origin and modification of insoluble organic matter in chondrites, the major source of Earth's C and N. *Chemie Der Erde-Geochemistry*. 77, 227-256.

Bones, D. L.; Carrillo Sánchez, J. D; Kulak, A. N.; Plane, J. M. C. (2019), Ablation of Ni from micrometeoroids in the upper atmosphere: experimental and computer simulations and implications for Fe ablation, *Planetary Space Science*, 179, art. no. 104725.

Carrillo-Sánchez, J. D.; Bones, D.; Douglas, K. M.; Flynn, G. J., Wirick, S., Fegley Jr., B.; Araki, T.; Kauliche, B.; Plane, J. M. C. (2020), Injection of meteoric phosphorus into planetary atmospheres, *Planetary Space Science*, 187, art. no. 104926.

Clemett, S. J., Sandford, S. A., Nakamura-Messenger, K., Horz, F., McKay, D. S. (2010), Complex aromatic hydrocarbons in Stardust samples collected from comet 81P/Wild 2. *Meteoritics & Planetary Science*. 45, 701-722.

Cody, G. D., et al. (2011), Establishing a molecular relationship between chondritic and cometary organic solids. *Proceedings of the National Academy of Sciences of the United States of America*. 108, 19171-19176.

Court, R. W., Sephton, M. A. (2009), Meteorite ablation products and their contribution to the atmospheres of terrestrial planets: An experimental study using pyrolysis-FTIR. *Geochimica et Cosmochimica Acta*. 73, 3512-3521.

Court, R. W., Sephton, M. A. (2011), The contribution of sulphur dioxide from ablating micrometeorites to the atmospheres of Earth and Mars. *Geochimica et Cosmochimica Acta*. 75, 1704-1717.

Flynn, G. J., Keller, L. P., Jacobsen, C., Wirick, S. (2004), An assessment of the amount and types of organic matter contributed to the Earth by interplanetary dust. In: M. P. Bernstein, M. Kress, R. NavarroGonzalez, (Eds.), *Space Life Sciences: Steps toward Origin(S) of Life*, pp. 57-66.

Flynn, G. J., Wirick, S., Keller, L. P. (2013), Organic grain coatings in primitive interplanetary dust particles: Implications for grain sticking in the Solar Nebula. *Earth Planets Space*. 65, 1159–1166.

Friend, P., Hezel, D. C., Barrat, J. A., Zipfel, J., Palme, H., Metzler, K. (2018), Composition, petrology, and chondrule-matrix complementarity of the recently discovered Jbilet Winselwan CM2 chondrite. *Meteoritics & Planetary Science*. 53, 2470-2491.

Gómez Martín, J. C.; D. L. Bones, J. D. Carrillo-Sánchez, A. D. James, J. M. Trigo-Rodríguez, B. Fegley Jr., and J. M. C. Plane (2017), Novel Experimental Simulations of the Atmospheric Injection of Meteoric Metals, *Astrophys. J.*, 836:, art. no. 212.

Hornung, K., et al. (2016), A first assessment of the strength of cometary particles collected in-situ by the COSIMA instrument onboard ROSETTA. *Planetary and Space Science*, 133, 63-75.

Janches, D.; Swarnalingam, N.; Carrillo-Sanchez, J. D.; Gómez-Martin, J. C.; Marshall, R.; Nesvorny, D.; Plane, J. M. C.; Feng, W.; Pokorny, P. (2017), Radar Detectability Studies of Slow and Small Zodiacal Dust Cloud Particles. III. The Role of Sodium and the Head Echo Size on the Probability of Detection, *Astrophysical Journal*, 843, art. no.: 1.

Jarosewich, E. (1990), *Chemical-Analyses of Meteorites: A compilation of stony and iron meteorite analyses*. *Meteoritics*. 25, 323-337.

Kimura, H., Hilchenbach, M., Merouane, S., Paquette, J., Stenzel, O. (2020), The morphological, elastic, and electric properties of dust aggregates in comets: A close look at COSIMA/Rosetta's data on dust in comet 67P/Churyumov-Gerasimenko. *Planetary and Space Science*, 181, art. 104825.

Mannel, T., M.S. Bentley, P.D. Boakes, H. Jeszenszky, P. Ehrenfreund, C. Engrand, C. Koeberl, A.C. Levasseur-Regourd, J. Romstedt, R. Schmied, K. Torkar, I. Weber (2019), Dust of comet 67P/Churyumov-Gerasimenko collected by Rosetta/MIDAS: classification and extension to the nanometre scale, *Astr. Astrophys.*, 630, A26.

Nozaki, W., Nakamura, T., Noguchi, T. (2006), Bulk mineralogical changes of hydrous micrometeorites during heating in the upper atmosphere at temperatures below 1000 degrees C. *Meteoritics & Planetary Science*. 41, 1095-1114.

Riebe, M. E. I., et al. (2020), The effects of atmospheric entry heating on organic matter in interplanetary dust particles and micrometeorites. *Earth and Planetary Science Letters*. 540, 116266.

Schramm, L. S., Brownlee, D. E., Wheelock, M. M. (1989), Major element composition of stratospheric micrometeorites. *Meteoritics*. 24, 99-112.

Thomas, K. L., Keller, L. P., Blanford, G. E., McKay, D. S. (1994), Quantitative-analyses of carbon in anhydrous and hydrated interplanetary dust particles. In: M. E. Zolensky, T. L. Wilson, F. J. M. Rietmeijer, G. J. Flynn, (Eds.), *Analysis of Interplanetary Dust*, pp. 165-172.

Thomas, E., J. Simolka, M. DeLuca, M. Horanyi, D. Janches, R. A. Marshall, T. Munsat, J.M.C. Plane, and Z. Sternovsky (2017), Experimental setup for the laboratory investigation of micrometeoroid ablation using a dust accelerator, *Rev. Sci. Instrum.* 88, 034501,